

Atomic Alchemy ¹

C. Greub and D. Wyler

Institut für Theoretische Physik, Universität Zürich
Zürich, Switzerland

and

S. J. Brodsky and C. T. Munger

Stanford Linear Accelerator Center
Stanford University, Stanford, California 94309

Abstract

We consider the transitions between electromagnetic bound states, such as the exclusive weak decay of a muonic atom into an electronic atom: $(\mu^- Z) \rightarrow (e^- Z)\bar{\nu}_e\nu_\mu$. We show that relativistic effects in the atomic wavefunctions are crucial for determining the rate. In the case of heavy atoms, the exclusive channel branching ratios exceed 10^{-6} , possibly bringing the study of these rare decays within experimental reach. Such processes thus provide a detailed laboratory for studying the high momentum tail of wavefunctions in atomic physics; in addition, they provide a simple toy model for investigating analogous exclusive heavy hadronic decays in quantum chromodynamics such as $B \rightarrow \pi e\nu$.

(Submitted to Physical Review D.)

¹Work partially supported by Schweizerischer Nationalfonds and the Department of Energy under contract DE-AC03-76SF00515.

1.) Introduction

The calculation of the rate of a weak decay of a heavy hadron into an exclusive channel, such as $B \rightarrow De\nu$ or $B \rightarrow \gamma K^*$, poses a challenging problem in nonperturbative quantum chromodynamics because all the complexities of the hadronic wavefunctions enter. In this paper we point out the possibility of studying an analogous, but far simpler process in atomic physics: the weak decay of one electromagnetic bound state into another. Simple examples occur in the decay of muonic atoms, such as

$$\begin{aligned} (\mu^- Z) &\rightarrow (e^- Z) \bar{\nu}_e \nu_\mu, \\ (\mu^+ e^-) &\rightarrow (e^+ e^-) \nu_e \bar{\nu}_\mu. \end{aligned} \quad (1)$$

Because the atom remains in a bound state, but the atomic or nuclear species is changed, we refer to such processes as “atomic alchemy.” We could also consider the decay $(\pi^+ e^-) \rightarrow (\mu^+ e^-) \nu_\mu$, or the decays of Coulomb-bound hadronic atoms such as $(\pi^- Z) \rightarrow (\mu^- Z) \bar{\nu}_\mu$ or $(\Sigma^- Z) \rightarrow (\bar{p} Z) \pi^0$; however, the observation of the latter transitions appears to be impractical because of the high rate at which hadrons are absorbed by the nucleus.

Other interesting examples of atomic alchemy occur when a nucleus is forced to change its state because of external scattering, while an atomic electron remains bound. The scattering may be due to neutron-induced fission, nuclear Compton scattering, or photodisintegration; the latter is particularly interesting for deuterium, $\gamma(d^+ e^-) \rightarrow (p^+ e^-) n$. One can also study atomic alchemy when a nucleus changes its state by an internal process, such as β -decay.

In this paper, we consider the exclusive transition $B_1 \rightarrow B_2 + X$, where both B_1 and B_2 are bound states consisting of particles $(b_1 s)$ and $(b_2 s)$, respectively, and the transition proceeds by the weak decay $b_1 \rightarrow b_2 + X$. The particle s will be called the spectator. We assume that there is an empty bound state in B_2 for the particle b_2 to settle in; in the detailed calculations given below we take this to be the ground state.

The basic features of atomic alchemy can be easily understood using non-relativistic mechanics; the analysis is similar to that for nuclear collisions involving capture of atomic electrons, as discussed, for example, by Migdal [1]. We review the major points before plunging into the full relativistic calculation. Because the weak decay occurs over a time short compared to the period of an orbit, we can use the “sudden approximation”. The probability amplitude for the atomic transition then factors into the free matrix element of the weakly decaying (moving) particle times a form factor $F(\vec{q}^2)$. This form factor is just the overlap of the wavefunctions of the initial and final states, which we write as ψ_1 and ψ_2 . In the rest frame of the initial state, $F(\vec{q}^2)$ is

$$F(\vec{q}^2) = \int \frac{d^3 k_1}{(2\pi)^3} \psi_1(\vec{k}_1) \psi_2^*(\vec{k}_2 = m_{red,2} \vec{v}_{rel,2}) \quad . \quad (2)$$

Here \vec{k}_1 is the momentum of b_1 (see Fig. 1), and $m_{red,2}$ and $\vec{v}_{rel,2}$ are the reduced mass and the relative velocity of the final state particles b_2 and s . The velocity $\vec{v}_{rel,2}$ is a function of \vec{q} , the momentum transfer carried by X , which by conservation of momentum is equal to the recoil momentum of B_2 . We have

$$\vec{v}_{rel,2} = \frac{\vec{k}_1 - \vec{q}}{m_{b_2}} + \frac{\vec{k}_1}{m_s} = \frac{\vec{k}_1}{m_{red,2}} - \frac{\vec{q}}{m_{b_2}} . \quad (3)$$

In the decay $(Z\mu^-) \rightarrow (Ze^-)\nu_\mu\bar{\nu}_e$, the argument \vec{k}_2 of the wavefunction ψ_2^* is approximately $\vec{k}_2 \approx \vec{k}_1 - \vec{q}$. In momentum space the muon wave function does not vary much over the domain where the electron wave function differs appreciably from zero. The integral in Eq. (2) can therefore be approximated by

$$F(\vec{q}^2) = \psi_1(\vec{q}) \psi_2^*(\vec{r} = 0) . \quad (4)$$

For small Z the momenta of both the muon and the electron are nonrelativistic and the effects of the finite nucleus size are small; we therefore can use for ψ_1 and ψ_2 the Schrödinger wavefunctions for a point nucleus. For the $1S$ states

$$\psi_i(\vec{k}) = \frac{8\sqrt{\pi}a_i^{3/2}}{[1 + a_i^2 k^2]^2} , \quad a_i = \frac{1}{m_{red,i}Z\alpha} , \quad (i = 1, 2) , \quad (5)$$

where a_i denote the Bohr-radii of the atoms. Because $\psi_i(\vec{r} = 0) = [\sqrt{\pi}a_i^{(3/2)}]^{-1}$, Eq. (4) becomes

$$F(\vec{q}^2) = 8 \left(\frac{m_e}{m_\mu} \right)^{3/2} \left[\frac{1}{1 + \vec{q}^2 / (Z\alpha m_\mu)^2} \right]^2 . \quad (6)$$

The physics of capture into a hydrogenic nS state is controlled by the ratio of the change in nuclear velocity to the atomic velocity $Z\alpha/n$. Equation (6) suggests that the highest rates for the transition of muonic to electronic atoms will be found for heavy nuclei with $(Z\alpha m_\mu)^2 \geq \vec{q}^2$. For these atoms, however, Eq. (6) provides only a very rough estimate for the form factor because relativistic effects (mainly affecting the wavefunction of the (Ze^-) atom) become crucial and greatly enhance the transition rate.

In the case of the transition $(\pi^+e^-) \rightarrow (\mu^+e^-)\nu_\mu$ the monoenergetic weak decay changes the species and velocity of the heavy particle serving as a nucleus. Since the momentum transfer from the pion to the muon is much larger than either Bohr momenta, the integrand in the form factor in Eq. (2) is dominated by those values of k_1 for which either k_1 or k_2 matches a Bohr momentum. Both contributions turn out to be equally important, and using for the $1S$ states the Schrödinger wavefunctions for a Coulomb potential, we obtain for the form factor

$$F(\vec{q}^2) \simeq 2\psi_1(\vec{r} = 0)\psi_2^*(m_{red,2}\vec{v}_{rel,2}) \simeq 16 \left(\frac{\alpha}{v_{rel,2}} \right)^4 . \quad (7)$$

Here $v_{rel,2} = (m_\pi^2 - m_\mu^2)/(2m_\pi m_\mu) = 0.28$, which is small enough that our non-relativistic treatment is justified. The probability for capture of the electron from the muonic decay is unfortunately very small:

$$P = [F(\vec{q}^2)]^2 \simeq 256\alpha^8/v_{rel,2}^8 \sim 5 \times 10^{-11} \quad . \quad (8)$$

2.) Relativistic Analysis of Atomic Transitions

We now turn to a more detailed analysis which allows us to treat decays such as $(Z\mu^-) \rightarrow (Ze^-)\nu_\mu\bar{\nu}_e$, where for large Z the velocities of the bound constituents are relativistic. In principle, the analysis requires a fully covariant description, such as the Bethe-Salpeter equation or the light-cone Fock state expansion. In Ref. [2] a covariant description was given, but at the expense of a somewhat artificial momentum-dependent mass for the decaying constituent. While that description works well when the decaying constituent is much heavier than the spectator, it fails when the spectator is the heavier particle, because the high momenta of the constituents, which prove crucial, are cut off (see Eq. (2.1) of Ref. [2]). Here we use a non-covariant description that is adequate for the cases of interest, where the spectators in the initial and final bound states have small relative velocity, but where the velocities of the particles bound to the spectators can be relativistic. This description is particularly appropriate for the transition $(\mu^- Z) \rightarrow (e^- Z) + \nu_\mu\bar{\nu}_e$ because the mass of a nucleus is much greater than m_μ .

We begin with a relativistic treatment of the simple, monoenergetic, two-body atomic transition $(\pi^+e^-) \rightarrow (\mu^+e^-) + \nu_\mu$. This is a close analog to the hadronic decay $B \rightarrow De\nu$. The relative velocity of the (πe) and (μe) systems is only $v_{rel} = 0.28$, so one can simplify the kinematics by assuming them to be at relative rest. We consider only S -wave bound states, so the spin of the bound state B_1 is just the spin of the electron, and the final bound state B_2 is either a pseudoscalar or a vector particle with the corresponding well-known spin combinations of the constituents. For example, the initial state B_1 with spin projection R is represented in its rest frame as

$$|B_1, \vec{p}_B = 0, R\rangle = \sqrt{2m_{B_1}} \int \frac{d^3k_1}{\sqrt{4k_1^0k_3^0}(2\pi)^3} \psi_1(\vec{k}_1) a_R^+(\vec{k}_1) b^+(\vec{k}_3) |0\rangle \quad , \quad (9)$$

where $\vec{k}_3 = -\vec{k}_1$, and $k_i^0 = (\vec{k}_i^2 + m_i^2)^{1/2}$ for $(i = 1, 3)$, and $a^+(\vec{k}_1)$ and $b^+(\vec{k}_3)$ are creation operators for the constituents that act on the vacuum state $|0\rangle$. The state is ‘‘covariantly’’ normalized in the volume V , so that

$$\langle B_1, \vec{p}_B = 0, R | B_1, \vec{p}_B = 0, S \rangle = 2m_{B_1} V \delta_{RS} \quad , \quad \text{if} \quad \int \frac{d^3k_1}{(2\pi)^3} |\psi_1(\vec{k}_1)|^2 = 1 \quad . \quad (10)$$

The matrix element for the decay $(\pi^+ e^-) \rightarrow (\mu^+ e^-) + \nu_\mu$ is then written as ²

$$M_{rs} = \frac{4G_F V_{ud}}{\sqrt{2}} \sqrt{4m_{B_1} m_{B_2}} \int \frac{d^3 k_1}{(2\pi)^3} \frac{\psi_1(\vec{k}_1)}{\sqrt{2k_1^0}} \frac{\psi_2^*(\vec{k}_2)}{\sqrt{2k_2^0}} S_{rs} \frac{f_\pi m_\pi}{2} \quad (11)$$

$$S_{rs} = \bar{u}_r(\vec{q}) \gamma_0 \frac{1 - \gamma_5}{2} v_s(\vec{k}_1 - \vec{q}) \quad , \quad k_2^0 = (m_\mu^2 + (\vec{k}_1 - \vec{q})^2)^{1/2} \quad , \quad (12)$$

where $f_\pi \approx 130$ MeV is the pion decay constant, and V_{ud} is the relevant CKM matrix element. Here $u_r(\vec{q})$ and $v_s(\vec{k}_1 - \vec{q})$ are the Dirac spinors of respectively the neutrino with spin r and the muon with spin s . The argument \vec{k}_2 of the bound state wavefunction ψ_2^* is given by $\vec{k}_2 = \vec{k}_1 - (m_{red,2}/m_\mu)\vec{q}$. Note that in S_{rs} we have kept only the zeroth component of the weak current since the pion is essentially at rest. In the limit $\vec{k}_1 - \vec{q} \ll m_\mu$, only the large components of the spinor need to be retained, and S_{rs} takes the simple form

$$S_{rs} = \frac{1}{2} \sqrt{2m_\mu |\vec{q}|} \left(\chi_r^+ \left(1 - \frac{\vec{\sigma} \cdot \vec{q}}{|\vec{q}|} \right) \varepsilon \chi_s \right) \quad ,$$

$$\varepsilon = i\sigma_2 \quad , \quad \chi_1^+ = (1, 0) \quad , \quad \chi_2^+ = (0, 1) \quad . \quad (13)$$

We square the matrix element, sum over pseudoscalar and vector final states, and average over the spin of the initial state. Using

$$\sum_{rs} S_{rs} S_{rs}^* = 2m_\mu |\vec{q}| \quad , \quad (14)$$

the spin-averaged matrix element becomes

$$\overline{|M|_\Sigma^2} = 4G_F^2 |V_{ud}|^2 f_\pi^2 m_\pi^2 |F(\vec{q}^2)|^2 m_\mu |\vec{q}|$$

$$F(\vec{q}^2) = \int \frac{d^3 k_1}{(2\pi)^3} \psi_1(\vec{k}_1) \psi_2^*(\vec{k}_2) \quad , \quad (15)$$

where we have used (see Eq. (11)) the approximation $4k_1^0 k_2^0 \approx 4m_{B_1} m_{B_2}$. The two-body kinematics fixes the momentum transfer $|\vec{q}|$ to be

$$|\vec{q}| = (m_{B_1}^2 - m_{B_2}^2)/(2m_{B_1}) \approx (m_\pi^2 - m_\mu^2)/(2m_\pi) \quad . \quad (16)$$

The decay rate in this approximation is

$$\Gamma = \frac{m_\pi^2 - m_\mu^2}{16\pi m_\pi^3} \overline{|M|_\Sigma^2} \quad . \quad (17)$$

To get an estimate of the errors made by using non-relativistic mechanics, we calculated the decay rate of a free pion making the same approximations, i.e. just

²We use spinors normalized as $\bar{u}_r(\vec{p}) u_s(\vec{p}) = -\bar{v}_r(\vec{p}) v_s(\vec{p}) = 2m\delta_{rs}$

taking the zeroth component of the weak current and retaining only the large components of the Dirac spinor of the muon. We find

$$\Gamma_{free}^{approx} = \frac{G_F^2 |V_{ud}|^2 f_\pi^2 m_\pi m_\mu (m_\pi^2 - m_\mu^2)^2}{8\pi m_\pi^3} . \quad (18)$$

This differs from the rate calculated using relativistic mechanics only by the factor

$$\Gamma_{free}^{exact} / \Gamma_{free}^{approx} = m_\pi / m_\mu \approx 1.3 , \quad (19)$$

which indicates a possible error of about 30%. The branching ratio for decay to the $1S$ state, obtained by dividing Eq. (17) by the approximate form in Eq. (18), is

$$\text{BR}((\pi^+ e^-) \rightarrow (\mu^+ e^-) \nu_\mu) = |F(\vec{q}^2)|^2 . \quad (20)$$

Using the Schrödinger wavefunctions of Eq. (5) (with $Z = 1$ of course) we have finally that $\text{BR}((\pi^+ e^-) \rightarrow (\mu^+ e^-) \nu_\mu) = 4.51 \times 10^{-11}$.

3.) Relativistic Effects in Muonic to Electronic Atom Decays

We now consider $(\mu^- Z) \rightarrow (e^- Z) \nu_\mu \bar{\nu}_e$, using with obvious replacements the same kinematics as in Fig. 1. For simplicity we will take the nucleus to be spinless. As we now consider a 3-body decay, we first discuss the ranges of the relevant kinematical variables. Because the two constituents have extremely different masses (especially if Z is large), it is useful to write the masses m_{B_1} and m_{B_2} of the bound states B_1 and B_2 in the form

$$\begin{aligned} m_{B_1} &= M + m_1 , \quad m_1 = m_\mu - E_{bind,1} ; \\ m_{B_2} &= M + m_2 , \quad m_2 = m_e - E_{bind,2} . \end{aligned} \quad (21)$$

Here M is the mass of the heavy nucleus. In the rest frame of the decaying atom, the momentum transfer $|\vec{q}|$ to the neutrino-pair is kinematically restricted to the range

$$0 \leq |\vec{q}| \leq (m_{B_1}^2 - m_{B_2}^2) / (2m_{B_1}) = (m_1 - m_2) + O(1/M) . \quad (22)$$

For a given value of $|\vec{q}|$, the fourth component q^0 as seen in the rest frame, and the square of the four-vector, q^2 , are fixed:

$$q^0 = (m_1 - m_2) + O(1/M), \quad q^2 = (m_1 - m_2)^2 - \vec{q}^2 . \quad (23)$$

Thus q^2 lies in the range $[0, (m_1 - m_2)^2]$. The momentum transfer $|\vec{q}|$ is always very small compared to the masses of the bound states, so the bound states can be considered to be at relative rest; in this approximation our formalism will still be

covariant up to $O(1/M)$ corrections. Writing the relevant four-Fermi operator for muon decay in charge retention form, the matrix element for the transition reads

$$M_{sr} = \frac{4G_F}{\sqrt{2}} \sqrt{4m_{B_1}m_{B_2}} N_\mu S_{sr}^\mu \quad , \quad (24)$$

where

$$N_\mu = \bar{u}(p_{\nu_\mu}) \gamma_\mu \frac{1 - \gamma_5}{2} v(p_{\nu_e}) \quad (25)$$

$$S_{sr}^\mu = \int \frac{d^3k_1}{(2\pi)^3} \psi_1(\vec{k}_1) \psi_2^*(\vec{k}_1 - \vec{q}) \frac{\bar{u}_s(e; \vec{k}_1 - \vec{q})}{\sqrt{2k_2^0}} \gamma^\mu \frac{1 - \gamma_5}{2} \frac{u_r(\mu; \vec{k}_1)}{\sqrt{2k_1^0}} \quad (26)$$

$$k_1^0 = \sqrt{m_\mu^2 + \vec{k}_1^2} \quad , \quad k_2^0 = \sqrt{m_e^2 + (\vec{k}_1 - \vec{q})^2} \quad . \quad (27)$$

The muon spin r and the electron spin s are just the spins of the bound states B_1 and B_2 . In general a Wigner rotation [2] must be used to relate spins in two different frames, but here the rotation is essentially unity because the relative velocity of B_1 and B_2 is small.

We seek an expression for M_{sr} that is correct to zeroth order in $1/M$. This is found most easily by first writing the trivial identity

$$S_{sr}^\mu = \delta_{ss'} S_{s'r'}^\mu \delta_{r'r} \quad , \quad (28)$$

and then by rewriting the Kronecker-deltas in terms of the spinors for the bound states and their constituents,

$$\begin{aligned} \delta_{r'r} &= \left(2m_{B_1}(k_1^0 + m_\mu)\right)^{-1/2} \bar{u}_{r'}(\mu; \vec{k}_1) u_r(B_1; \vec{0}) \quad , \\ \delta_{ss'} &= \left(2m_{B_2}(k_2^0 + m_e)\right)^{-1/2} \bar{u}_s(B_2; \vec{p}_{B_2}) u_{s'}(e; \vec{k}_1 - \vec{q}) \quad . \end{aligned} \quad (29)$$

The first relation is exact, and the second introduces errors only $O(1/M)$. Then S_{sr}^μ can be written as

$$S_{sr}^\mu = (4m_{B_1}m_{B_2})^{-1/2} \bar{u}_s(B_2; \vec{p}_{B_2}) T^\mu u_r(B_1; \vec{0}) \quad , \quad (30)$$

where T^μ may be derived using eqs. (26), (28), and (29). By repeatedly using the Dirac equations

$$\gamma^0 u_r(B_1; \vec{0}) = u_r(B_1; \vec{0}) \quad , \quad \bar{u}_s(B_2; \vec{p}_{B_2}) \gamma^0 = \bar{u}_s(B_2; \vec{p}_{B_2}) + O(1/M) \quad , \quad (31)$$

and dropping terms $\sim q^\mu$, which vanish when contracting with the neutrino tensor N_μ of Eq. (25), we arrive after some not completely straightforward algebra at

$$T^\mu = F_1(q^2) \gamma^\mu L + F_2(q^2) \gamma^\mu R + F_3(q^2) \gamma^\mu \frac{\not{q}}{m_\mu} L + F_4(q^2) \gamma^\mu \frac{\not{q}}{m_\mu} R \quad . \quad (32)$$

Here $L = (1 - \gamma_5)/2$, and $R = (1 + \gamma_5)/2$, and the form factors $F_i(q^2)$ are given as

$$F_i(q^2) = \int \frac{d^3 k_1}{(2\pi)^3} \psi_1(\vec{k}_1) \psi_2^*(\vec{k}_1 - \vec{q}) \frac{h_i}{\sqrt{4k_1^0 k_2^0 (k_1^0 + m_\mu)(k_2^0 + m_e)}} , \quad (33)$$

with

$$\begin{aligned} h_1 &= (k_1^0 + m_\mu)(k_2^0 + m_e) + q^0 \left[(1 - C)(k_1^0 + m_\mu) - C(k_2^0 + m_e) \right] \\ &\quad + (B - C)(q^0)^2 - A \\ h_2 &= (C - B)q^2 - 2A \\ h_3 &= \left[(1 - C)(k_1^0 + m_\mu) + (B - C)q^0 \right] m_\mu \\ h_4 &= \left[C(k_2^0 + m_e) - (B - C)q^0 \right] m_\mu . \end{aligned} \quad (34)$$

The quantities A , B , and C are

$$A = \frac{\vec{q}^2 \vec{k}_1^2 - (\vec{k}_1 \cdot \vec{q})^2}{2\vec{q}^2} , \quad B = \frac{3(\vec{k}_1 \cdot \vec{q})^2 - \vec{q}^2 \vec{k}_1^2}{2(\vec{q}^2)^2} , \quad C = \frac{\vec{k}_1 \cdot \vec{q}}{\vec{q}^2} . \quad (35)$$

The form factors F_i may seem non-covariant, because after the integration $d^3 \vec{k}_1$ the variables q^0 and $|\vec{q}|$ remain as well as the square of the four-momentum, q^2 . But the form factors were derived in the rest frame of B_1 , so q^0 and $|\vec{q}|$ are functions only of q^2 according to Eq. (23).

In terms of the quantities introduced, the matrix element can be written in the suggestive form

$$M_{sr} = \frac{4G_F}{\sqrt{2}} \bar{u}(p_{\nu_\mu}) \gamma_\mu L v(p_{\nu_e}) \bar{u}_s(B_2; \vec{p}_{B_2}) T^\mu u_r(B_1; \vec{0}) . \quad (36)$$

The calculation of the decay rate, differential in the momentum transfer $|\vec{q}|$, is now standard. Expressing the bound state masses m_{B_1} and m_{B_2} in terms of M , m_1 , and m_2 as defined in Eq. (21), one obtains

$$\begin{aligned} \frac{d\Gamma}{d|\vec{q}|} &= \frac{G_F^2 |\vec{q}|^2}{12\pi^3} K(|\vec{q}|) \\ K(|\vec{q}|) &= [q^2 + 2(m_1 - m_2)^2] (F_1^2 + F_2^2) + \frac{q^2}{m_\mu^2} [4(m_1 - m_2)^2 - q^2] (F_3^2 + F_4^2) \\ &\quad - 6q^2 \left[F_1 F_2 + \frac{q^2}{m_\mu^2} F_3 F_4 + \frac{m_1 - m_2}{m_\mu} (F_1 - F_2) (F_3 - F_4) \right] , \end{aligned} \quad (37)$$

where the F_i are the form factors defined in Eq. (33). Note that m_1 and m_2 enter only through their difference; this is clear from the decomposition (21), which is invariant under the change of variables $M \rightarrow M + \lambda$ and $m_i \rightarrow m_i - \lambda$.

The wavefunctions that enter the form factors F_i in Eq. (33) are plotted in Figs. 2 and 3 (solid line). For comparison we have also drawn the wavefunctions for a point

nucleus. The finite size of the nucleus affects the muon $1S$ wavefunction at high Z , as shown in Fig. 2. The finite size also affects the ultra-relativistic momentum tail of the electron $1S$ wavefunction, as shown in Fig. 3. The calculation of these wavefunctions is discussed in detail in the appendix. Briefly, we have approximated the shape of a nucleus of atomic number A as a homogeneously charged sphere of radius $r_0 = 1.3 A^{1/3}$ fm. In position space we solve the Dirac equation inside and outside r_0 ; the condition that these solutions match at $r = r_0$ determines the ground state wavefunction. We then take its Fourier transform.

From the kinematics (see Eq. (22)) it is clear that the muon $1S$ wavefunction is tested to momenta the order of m_μ . As shown in Fig. 2, relativistic effects are moderate. However, the finite size of the nucleus enhances the low momentum part of the muon wavefunction, which is fortunate because for lower momenta the electron wavefunction is large, and so the overlap increases. The electron $1S$ wavefunction is also tested up to momenta the order of m_μ and so the ultra-relativistic tail of the Dirac wavefunction is important. As shown in Fig. 3 the finite size of the nucleus diminishes the tail, and so the overlap with muon wavefunction decreases. At high Z we find that while the shape of the spectrum in $|\vec{q}|$ is altered, the increase and the decrease in the total rate due to the finite nuclear size balance remarkably, giving the same predicted total rate for atomic alchemy as does a calculation using a point nucleus.

Using the same approximations we also calculate the free-electron decay rate $\Gamma_{e,free}$ for $(Z\mu^-)$ decays. We write the mass of the bound state B_1 as $m_{B_1} = M + \hat{\gamma}m_\mu$, so that $\hat{\gamma}m_\mu$ is the total energy of the muon (see Eq. (22)). We find

$$\Gamma_{e,free} = \Gamma^0 \hat{\gamma}^2 \langle L^{-1} \rangle, \quad \langle L^{-1} \rangle = \int \frac{d^3k_1}{(2\pi)^3} |\psi_1(\vec{k}_1)|^2 \frac{m_\mu}{\sqrt{k_1^2 + m_\mu^2}}, \quad (38)$$

where $\Gamma^0 = G_F^2 m_\mu^5 / (192\pi^3)$ is the decay width of a free muon, and $\langle L^{-1} \rangle$ can be interpreted as the mean inverse Lorentz factor representing the slowing of the muon decay rate due to its orbital velocity. Numerically, we have $\langle L^{-1} \rangle = 0.96$, for $Z = 80$ and $A = 200$; and $\langle L^{-1} \rangle = 1.00$, for $Z = 10$ and $A \leq 20$. For $Z = 80$ and $A = 200$, numerically $\hat{\gamma}$ is 0.91; for a point nucleus with $Z = 80$ note that $\hat{\gamma}$ and $\langle L^{-1} \rangle$ are significantly smaller, $\hat{\gamma} = (1 - (Z\alpha)^2)^{1/2} = 0.81$ and $\langle L^{-1} \rangle = 0.85$. However, for $Z \approx 80$, muon capture dominates the free-electron decay by a factor of about 30 [3]. The branching ratio is now obtained by numerically integrating the spectrum in Eq. (37) and dividing by $\Gamma_{tot} = 30 \times \Gamma_{e,free}$, with $\Gamma_{e,free}$ given in Eq. (38). Using Dirac wavefunctions, the results for $Z = 80$ are

$$\begin{aligned} BR[(Z\mu^-) \rightarrow (Ze^-)\nu_\mu\bar{\nu}_e] &= 1.19 \times 10^{-6}, \text{ (finite nucleus, } A = 200), \\ BR[(Z\mu^-) \rightarrow (Ze^-)\nu_\mu\bar{\nu}_e] &= 1.19 \times 10^{-6}, \text{ (point nucleus)}. \end{aligned} \quad (39)$$

We note that the effects of the finite size of the nucleus do influence the shape of the momentum spectrum $d\Gamma/d|\vec{q}|$, as shown in Fig. 4, but that they leave the total rate essentially unchanged even for Z as large as 80. As the finite size effects are

expected to be smaller for smaller Z , we can calculate the rate for $Z = 10$ using the Dirac wavefunctions for a point nucleus. We get now, assuming \approx equal rates for capture and free-electron decay

$$BR[(Z\mu^-) \rightarrow (Ze^-)\nu_\mu\bar{\nu}_e] = 1.25 \times 10^{-9} , \text{ (point nucleus, } Z = 10) . \quad (40)$$

To appreciate the relativistic enhancement due to the Dirac wavefunctions, we also show the result obtained with the Schrödinger wavefunctions for a point nucleus:

$$\begin{aligned} BR[(Z\mu^-) \rightarrow (Ze^-)\nu_\mu\bar{\nu}_e] &= 2.32 \times 10^{-8} , \text{ (} Z = 80) , \\ BR[(Z\mu^-) \rightarrow (Ze^-)\nu_\mu\bar{\nu}_e] &= 9.32 \times 10^{-10} , \text{ (} Z = 10) . \end{aligned} \quad (41)$$

The relativistic enhancement for $Z = 80$ is a remarkable factor of 50.

In Fig. 4 the decay distribution $d\Gamma/d|\vec{q}|$, divided by the total width Γ_{tot} , is given for $Z = 80$. For illustration we also give the spectra predicted using the Schrödinger and Dirac wavefunctions for a point nucleus. Comparing these two curves shows that relativistic effects not only change the overall normalization but cause the spectrum to peak at higher momenta. The finite nuclear size causes the shape of the spectrum as calculated for a point nucleus to narrow. This can easily be understood by looking at the muonic wavefunction in Fig. 2. In Fig. 5 the same distribution is shown for $Z = 10$; as might be expected both relativistic effects and the effect of a finite nuclear size are small. Transitions of the form $(Z\mu) \rightarrow (Ze) + \nu\bar{\nu}$ have as their signature a bound state recoiling with a large momentum the order of m_μ . The momentum distribution for heavy atoms ($Z = 80$) peaks at about 20 MeV as seen in Fig. 4.

4.) Conclusions

In this paper we have shown that transitions between electromagnetic bound states can be calculated reliably using relativistic atomic wavefunctions. The rates and also the shapes of the spectra depend drastically on relativistic corrections; for heavy muonic atoms these enhance the branching ratio to a sizeable value of $\sim 10^{-6}$ from $\sim 10^{-8}$ (see Eqs. (39) and (41)). The QED analysis of these alchemy transitions illustrates some of the physics of the relativistic wavefunctions that must invariably enter the QCD analysis of the corresponding exclusive electroweak decays of hadrons.

Prospects for an experimental test of atomic alchemy are dim but not hopeless. While the branching ratio appears to be too small to be detectable for (πe) or for light muonic atoms, it may be possible to detect it for heavy muonic atoms. One promising approach is to inject and capture ~ 5 keV muons in a cyclotron trap [4] containing ~ 0.1 bar of a noble gas, which we will here assume to be neon ($Z = 10$). The muons will come to rest [4] in $\sim 1 \mu\text{s}$ and be captured by a neon atom. The muons will rapidly cascade to the $1S$ state, mostly by the ejection of atomic electrons. In neon the mean number of electrons in the K shell has been measured [5] to lie

between 0.07 and 0.68 by the time the muon has fallen to states with principal quantum number $n = 5$, in agreement with simple estimates [6] of 0.25, and will certainly diminish further as the muon continues to the $1S$ state. Total ionization of an atom has been observed in the cascades of antiprotons in neon, argon, and krypton [7]. The electron K shell will therefore be vacant to receive the electron from atomic alchemy. Only 0.31 of the muons in the $1S$ state of neon will be lost to muon capture [8], so most of the captured muons will be available to decay by atomic alchemy. At a pressure of ~ 0.1 bar, using estimates in [6] for the velocity of muonic neon ion ($\sim 10^5$ cm/s) and for the cross section for electron capture for Ne^{9+} on Ne ($\sim 3 \cdot 10^{-15}$ cm²), the time taken for a bare neon atom to capture an electron is the order of $1 \mu\text{s}$, so most of the captured muons will decay before the electron K shell can refill and block the atomic alchemy. It has been suggested [5] that cyclotron traps, admittedly with higher gas pressures, can be built capable of stopping $\sim 10^7 \mu^-/\text{s}$, so a branching ratio as small as $\sim 10^{-9}$ might be accessible.

Even if such a system could be realized the experimental difficulties would be daunting. The signature for atomic alchemy is the appearance of $^{20}\text{Ne}^{9+}$ ions with a distribution dN/dq^2 extending to a momentum the order of m_μ . These ions will be difficult to distinguish from $^{20}\text{F}^{9+}$ ions with a momentum of m_μ made by internal conversion. Nor will it be easy to extract the ions for analysis because in 0.1 bar of Neon the distance a bare ion can fly before capturing an electron is only ~ 1 mm, and the gas pressure cannot be lowered without letting the muons in the trap decay in flight before they can be captured. However, measurement of the spectrum dN/dq^2 would be valuable; it directly reflects the local structure of the atomic momentum space wavefunction and the beta decay spectrum. This appears to be one of the few ways in which one can directly study the relativistic tail of bound state wavefunctions in QED.

For induced reactions, such as $\gamma(d^+e^-) \rightarrow (p^+e^-)n$, one will observe a nearly monoenergetic final state hydrogen atom recoiling against an outgoing neutron. In principle one can use the doppler-shifted radiation from the outgoing atoms as a precise calibration of the nuclear scattering kinematics. One could also analyze the spin states of the outgoing atomic system and its hyperfine spectrum as a probe of the spin state of the final state nucleus.

We would like to thank P. Truöl, R. Engfer, I.B. Khriplovich, and M. Strikman for stimulating discussions.

References

- [1] A. B. Migdal, “Qualitative Methods in Quantum Theory”, Benjamin, 1977, (Frontiers in Physics series, 48).
- [2] C. Greub and D. Wyler, Phys. Lett. **B295** (1992) 293.

- [3] See “Weak Interaction Physics”, C. Rubbia, in “High Energy Physics,” E.H.S. Burhop, ed., Academic Press, New York, 1969, Table VI.
- [4] L. M. Simons, in “Fundamental Symmetries”, P. Bloch, ed., p. 89, Plenum Press, New York, 1987. See also [5].
- [5] R. Bacher, P. Blüm, D. Gotta, K. Heitlinger, and M. Schneider, Phys. Rev. A**39**, 1610 (1989).
- [6] R. Bacher, D. Gotta, L. M. Simons, J. Missimer, and N. M. Mukhopadhyay, Phys. Rev. Lett. **54**, 2087 (1985).
- [7] R. Bacher, P. Blüm, D. Gotta, K. Heitlinger, M. Schneider, J. Missimer, L. M. Simons, and K. Elsener, Phys. Rev. A**38**, 4395 (1988).
- [8] J. L. Rosen, E. W. Anderson, E. J. Bleser, L. M. Lederman, S. L. Meyer, J. E. Rothberg, and I. T. Wang, Phys. Rev. **132**, 2691 (1963).
- [9] J. D. Bjorken and S. D. Drell, “Relativistic Quantum Mechanics”, International Series in Pure and Applied Physics, McGraw-Hill Company, New York.
- [10] H. Behrends and W. Bühring, “Electron Radial Wave Functions and Nuclear Beta-decay”, International Series of Monographs on Physics, Vol. 67, Clarendon Press, Oxford 1982.
- [11] L. D. Landau, E. M. Lifschitz, “Course of Theoretical Physics, Volume 4: Quantum Electrodynamics” , Pergamon Press, Oxford.
- [12] M. Abramowitz and A. Stegun, “Handbook of Mathematical Functions”, Dover Publications, Inc., New York.
- [13] I.B. Khriplovich, “Parity Nonconservation in atomic Phenomena”, Gordon and Breach, 1991.

Figure captions

Figure 1

General diagram for a weak alchemy transition $B_1 \rightarrow B_2 + X$ as discussed in the text. The momenta of the particles are indicated in parentheses.

Figure 2

Schrödinger and Dirac wavefunctions (multiplied by $|\vec{k}|$) for a $(Z\mu^-)$ atom with $Z=80$.

Figure 3

Schrödinger and Dirac wavefunctions (multiplied by $|\vec{k}|$) for a (Ze^-) atom with $Z=80$.

Figure 4

Decay spectrum $d\Gamma/d|\vec{q}|$ divided by $\Gamma_{tot} = 30 \times \Gamma_{e,free}$ (Eq. (38)) for $Z=80$ (see text). The full line is obtained by using Dirac wavefunctions which take into account the finite size of the nucleus. The dashed (dashed-dotted) line corresponds to point-like Dirac (Schrödinger) wavefunctions. The curve based on Schrödinger wavefunctions is multiplied by a factor 50.

Figure 5

Decay spectrum $d\Gamma/d|\vec{q}|$ divided by $\Gamma_{tot} = 2 \times \Gamma_{e,free}$ (Eq. (38)) for $Z=10$ (see text). The full (dashed) line corresponds to point-like Dirac (Schrödinger) wavefunctions.

Appendix: Dirac wavefunctions

In atomic alchemy $(Z\mu) \rightarrow (Ze)\nu_\mu\bar{\nu}_\mu$ the electron wavefunction is probed at momenta the order of m_μ . Schrödinger wave functions are not appropriate and the Dirac wavefunctions [9] must be used. Recoil corrections due to the finite nuclear mass are extremely small, so the Dirac wavefunctions for an electron in the field of an infinitely heavy nucleus will describe adequately the high momentum tail of the electron (and muon) wavefunction. At large Z the Bohr radius of the muon $1S$ state is less than the nuclear radius, so the effect of the finite size of the nucleus on the muon wavefunction must obviously be included; the effect of the finite size is also important on the high-momentum tail of the electron $1S$ wavefunction.

We sketch how the momentum-space wavefunctions $\psi_1(\vec{k})$ and $\psi_2(\vec{k})$ that appear in the form factors in Eq. (33) are extracted from the usual 4-component Dirac wavefunctions in position space. Because everything can be worked out analytically for a point nucleus, we describe this case first.

Point nucleus

From the literature (e.g. from [9] on page 55) we take the (four component) ground state wave function in position space, $\psi_{n=1,j=1/2,j_z=1/2}(r, \theta, \phi)$. For brevity we write this as $\Phi(\vec{x})$. Taking the Fourier transform, we get the wavefunction in momentum space,

$$\tilde{\Phi}(\vec{k}) = \int d^3x \Phi(\vec{x}) \exp(-i\vec{k} \cdot \vec{x}) \quad , \quad (42)$$

$$\tilde{\Phi}(\vec{k}) = \begin{pmatrix} \hat{f}(k) \begin{pmatrix} 1 \\ 0 \end{pmatrix} \\ \hat{g}(k) \frac{\vec{\sigma} \cdot \vec{k}}{k} \begin{pmatrix} 1 \\ 0 \end{pmatrix} \end{pmatrix}, \quad k = |\vec{k}|, \quad (43)$$

with

$$\hat{f}(k) = \frac{N}{k(1+a^2k^2)^{1+\gamma/2}} (\sin \rho + ak \cos \rho) \quad (44)$$

$$\hat{g}(k) = \frac{Nm(1-\gamma)}{\gamma k^2(1+a^2k^2)^{1+\gamma/2}} \left[(1+(1+\gamma)a^2k^2) \sin \rho - \gamma ak \cos \rho \right] \quad (45)$$

$$a = \frac{1}{mZ\alpha}, \quad \gamma = \sqrt{1-(Z\alpha)^2}, \quad \rho = \gamma \operatorname{atan}(ak), \quad N = 2^{\gamma+1} \Gamma(1+\gamma) \sqrt{\frac{a\pi(1+\gamma)}{\Gamma(1+2\gamma)}}. \quad (46)$$

Here m denotes the reduced mass of the system, which we take to be identical to that of the muon or the electron because we work to lowest order in $1/M$. The corresponding energy eigenvalue is then $E = m\gamma$. For $Z = 80$ the numerical value of γ is 0.81.

The Dirac wavefunction for a bound state of course projects onto plane waves of both positive and negative energies; the latter waves correspond to antiparticles. We therefore define the relevant wavefunction (to be used in calculating the form factors) by the projection on positive energy plane waves. Thus we expand $\tilde{\Phi}(\vec{k})$ in terms of spinors $u_r(\vec{k})$ and $v_r(-\vec{k})$, writing

$$\tilde{\Phi}(\vec{k}) = \sum_r \left[A_r(\vec{k}) \frac{u_r(\vec{k})}{\sqrt{2k^0}} + B_r^*(-\vec{k}) \frac{v_r(-\vec{k})}{\sqrt{2k^0}} \right], \quad k^0 = \sqrt{\vec{k}^2 + m^2}. \quad (47)$$

If $j_z = 1/2$ we get

$$\begin{aligned} A_{+1/2}(\vec{k}) &= \sqrt{\frac{k^0+m}{2k^0}} \left(\hat{f}(k) + \frac{k}{k^0+m} \hat{g}(k) \right); \quad A_{-1/2} = 0; \quad (48) \\ B_{+1/2}^*(-\vec{k}) &= -\sqrt{\frac{k^0+m}{2k^0}} \frac{(k^1+ik^2)}{k} \left(\frac{k}{k^0+m} \hat{f}(k) - \hat{g}(k) \right) \\ B_{-1/2}^*(-\vec{k}) &= \sqrt{\frac{k^0+m}{2k^0}} \frac{k^3}{k} \left(\frac{k}{k^0+m} \hat{f}(k) - \hat{g}(k) \right) \end{aligned}$$

Here $A_r(\vec{k})$ is the probability amplitude to find an electron with momentum \vec{k} and spin r in the atom, while $B_r^*(-\vec{k})$ is the probability amplitude to find a positron with momentum \vec{k} and spin r ; the latter amplitude arises from the creation of e^+e^- pairs on the nucleus. Because the wave function in position space is normalized

as $\int d^3x \Phi^+(\vec{x}) \Phi(\vec{x}) = 1$, the Fourier transform is automatically normalized as $\int d^3k/(2\pi)^3 \tilde{\Phi}^+(\vec{k}) \tilde{\Phi}(\vec{k}) = 1$. Therefore $A_r(\vec{k})$ and $B_r^*(-\vec{k})$ are normalized so that

$$\int \frac{d^3k}{(2\pi)^3} \sum_r \{|A_r(\vec{k})|^2 + |B_r(\vec{k})|^2\} = 1 \quad . \quad (49)$$

The integral $\int d^3k/(2\pi)^3 \sum_r |B_r(\vec{k})|^2$ gives the probability to find a three particle Fock state ($e^+e^-e^-$) in the atom. Even for $Z = 80$ this fraction is tiny ($\approx 0.2\%$), so we only consider the one-Fock contribution characterized by $A_r(\vec{k})$. We mention that if we consider the atom with $j_z = -1/2$, we get $A_{+1/2}(\vec{k}) = 0$, and $A_{-1/2}(\vec{k})$ is identical to $A_{+1/2}(\vec{k})$, given in Eq. (48) for $j_z = +1/2$. The wavefunction denoted in the text as $\psi(\vec{k})$ is therefore given in the relativistic case by

$$\psi(\vec{k}) = A_{+1/2}(\vec{k}) \quad . \quad (50)$$

Because the coefficients B_r are very small, the effects of antiparticle production are small, and we get essentially the same form factor as we would have got had we naively computed the simple overlap of the wavefunctions in position space.

Finite-size nucleus

As usual (see e.g. [10]), we model a nucleus of atomic number A as a homogeneously charged sphere of radius $r_0 = 1.3 A^{1/3}$ fm; numerically $r_0 \approx 7$ fm for $A = 200$. Inside the sphere the potential has the form $V(r) = -(Z\alpha/r_0) \cdot (3 - r^2/r_0^2)/2$, and outside we have $V(r) = -Z\alpha/r$. In the notation of Landau-Lifschitz [11] we write the four-component Dirac function $\Phi(\vec{r})$ as

$$\Phi(\vec{r}) = N \begin{pmatrix} f(r) \begin{pmatrix} 1 \\ 0 \end{pmatrix} \\ -ig(r) \frac{\vec{\sigma} \cdot \vec{r}}{r} \begin{pmatrix} 1 \\ 0 \end{pmatrix} \end{pmatrix}, \quad r = |\vec{r}|, \quad (51)$$

where the constant N is chosen such that $\int d^3r \Phi^+(\vec{r}) \Phi(\vec{r}) = 1$. The radial equations for f and g are

$$\begin{aligned} f'(r) - (E + m - V(r))g(r) &= 0 \\ g'(r) + \frac{2}{r}g(r) + (E - m - V(r))f(r) &= 0 \end{aligned} \quad (52)$$

which are solved separately in the two regions $r \leq r_0$ and $r \geq r_0$ for an arbitrary constant $E < m$. In the outer region $r \geq r_0$ there is (up to an overall constant) exactly one solution (f, g) that is square integrable at $r = \infty$. It is given by (see Landau-Lifschitz [11])

$$f(r) = \sqrt{m + E} \exp(-\lambda r) r^{\gamma-1} (Q_1 + Q_2)$$

$$\begin{aligned}
g(r) &= -\sqrt{m-E} \exp(-\lambda r) r^{\gamma-1} (Q_1 - Q_2) \\
Q_1 &= U\left(\gamma - \frac{Z\alpha E}{\lambda}, 2\gamma + 1, 2\lambda r\right) \\
Q_2 &= -\left(1 - \frac{Z\alpha m}{\lambda}\right) U\left(\gamma + 1 - \frac{Z\alpha E}{\lambda}, 2\gamma + 1, 2\lambda r\right) \\
\lambda &= \sqrt{m^2 - E^2} \quad , \quad \gamma = \sqrt{1 - (Z\alpha)^2} \quad .
\end{aligned} \tag{53}$$

The hypergeometric function U is defined and discussed in detail in chapter 13 of Abramowitz-Stegun [12]; it is also related to Whittaker functions which are numerically accessible in the CERN-library.

In the inner region ($r \leq r_0$) a simplified solution for the (massless) electron has been obtained by Khriplovich [13]; however, the substantial mass of the muon requires a more complete treatment. It turns out that the Dirac equation has (again up to an overall constant) exactly one solution (f, g) that is square integrable at $r = r_0$; in the present case it has a Taylor series expansion around $r = 0$. While f starts as a constant, g begins with a term linear in r . The coefficients of the power series expansions of f and g may be defined recursively.

The inner and outer solutions must satisfy the matching condition

$$(f/g)_{r \rightarrow r_{0-}} = (f/g)_{r \rightarrow r_{0+}} \tag{54}$$

in order to be solutions of the complete equation. This can only hold for certain values of E ; these are just the eigenvalues. For $Z = 80$ and $A = 200$ the lowest eigenvalues are $E = 0.908m_\mu$ and $E = 0.811m_e$ for the $1S$ states of the muon and the electron, respectively.

The Fourier transform $\tilde{\Phi}(\vec{k})$ is then defined and written in terms of $\hat{f}(k)$ and $\hat{g}(k)$ precisely as in eqs. (42) and (43). Proceeding through the same steps as for a point nucleus, one finally gets the wavefunction $\psi(\vec{k})$ (compare with Eq. (50)) in a numerical form. This wavefunction shown for the $(Z\mu)$ and the (Ze) atoms in Figs. 2 and 3, respectively.

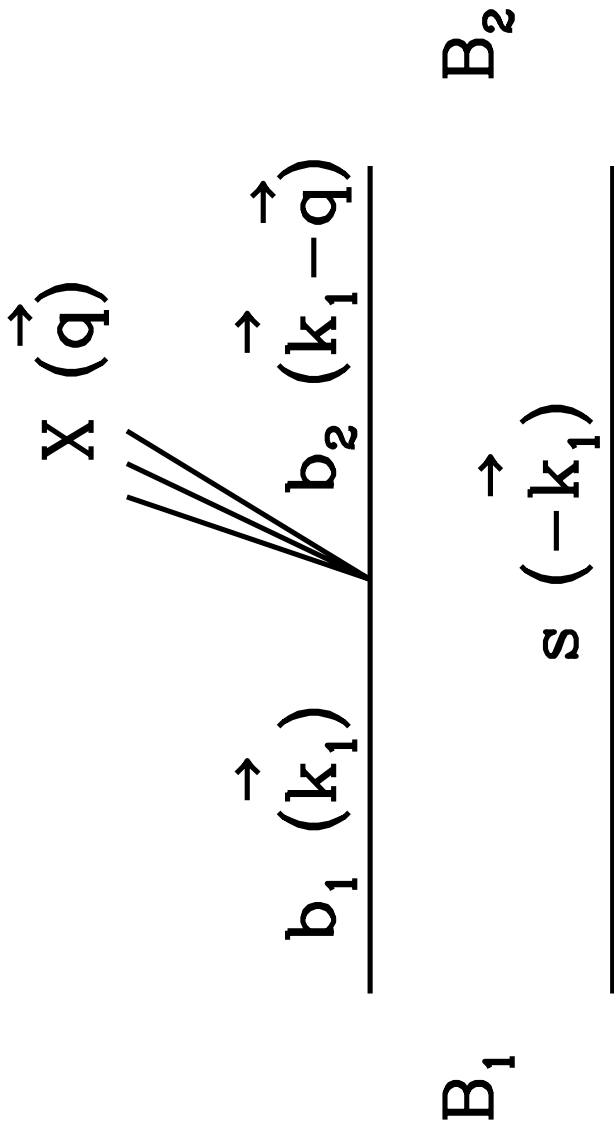


Fig. 1

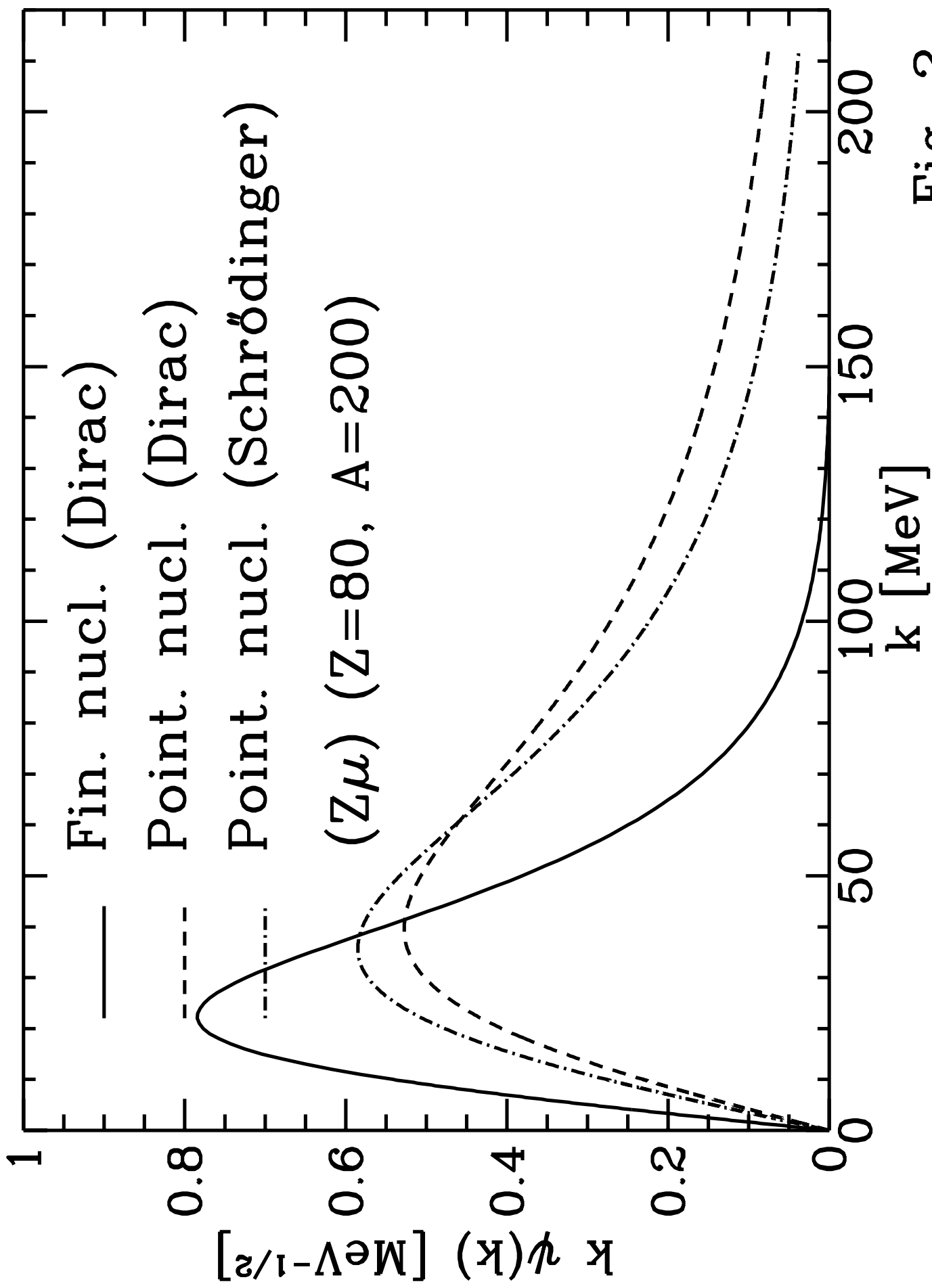


Fig. 2

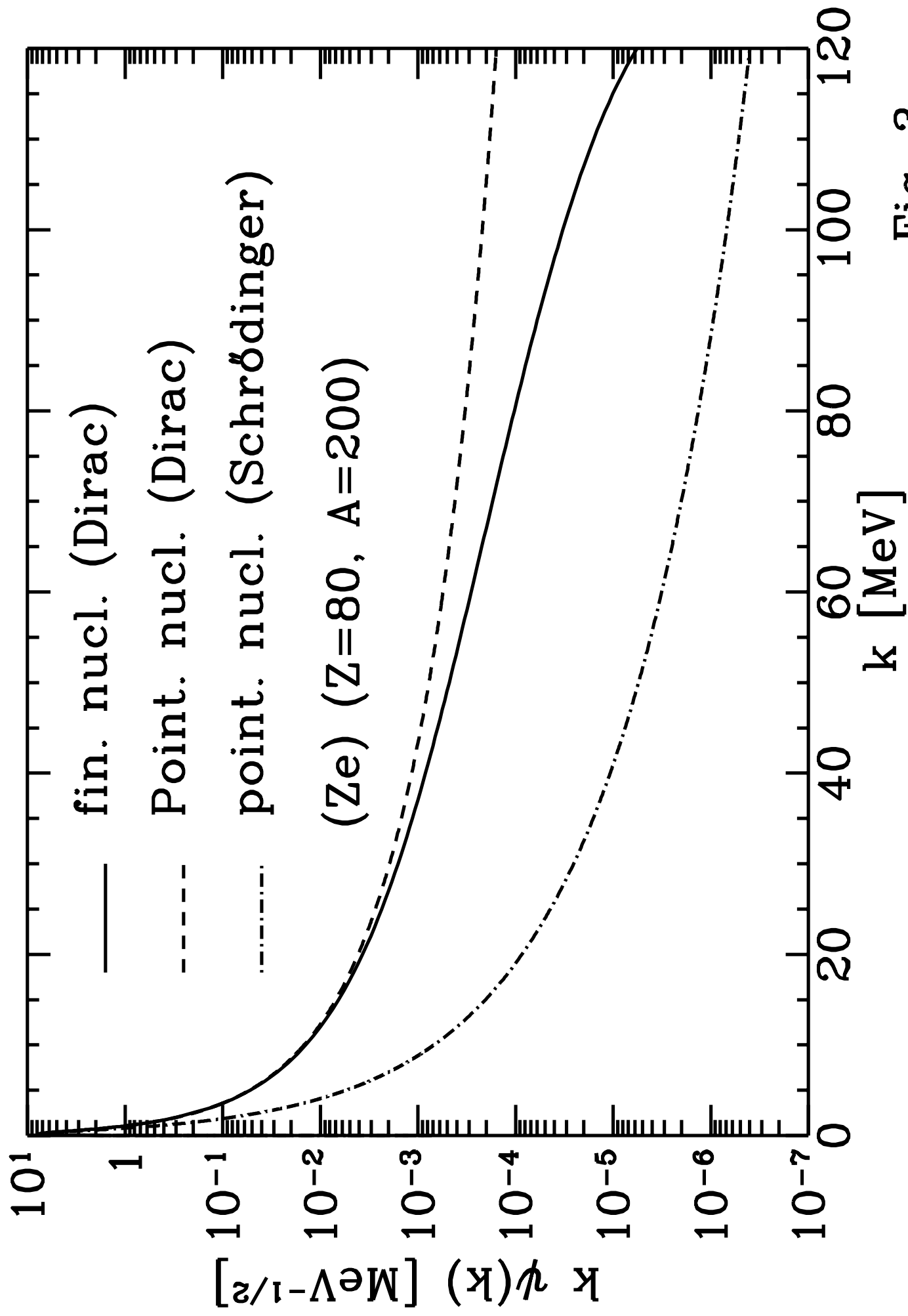


Fig. 3

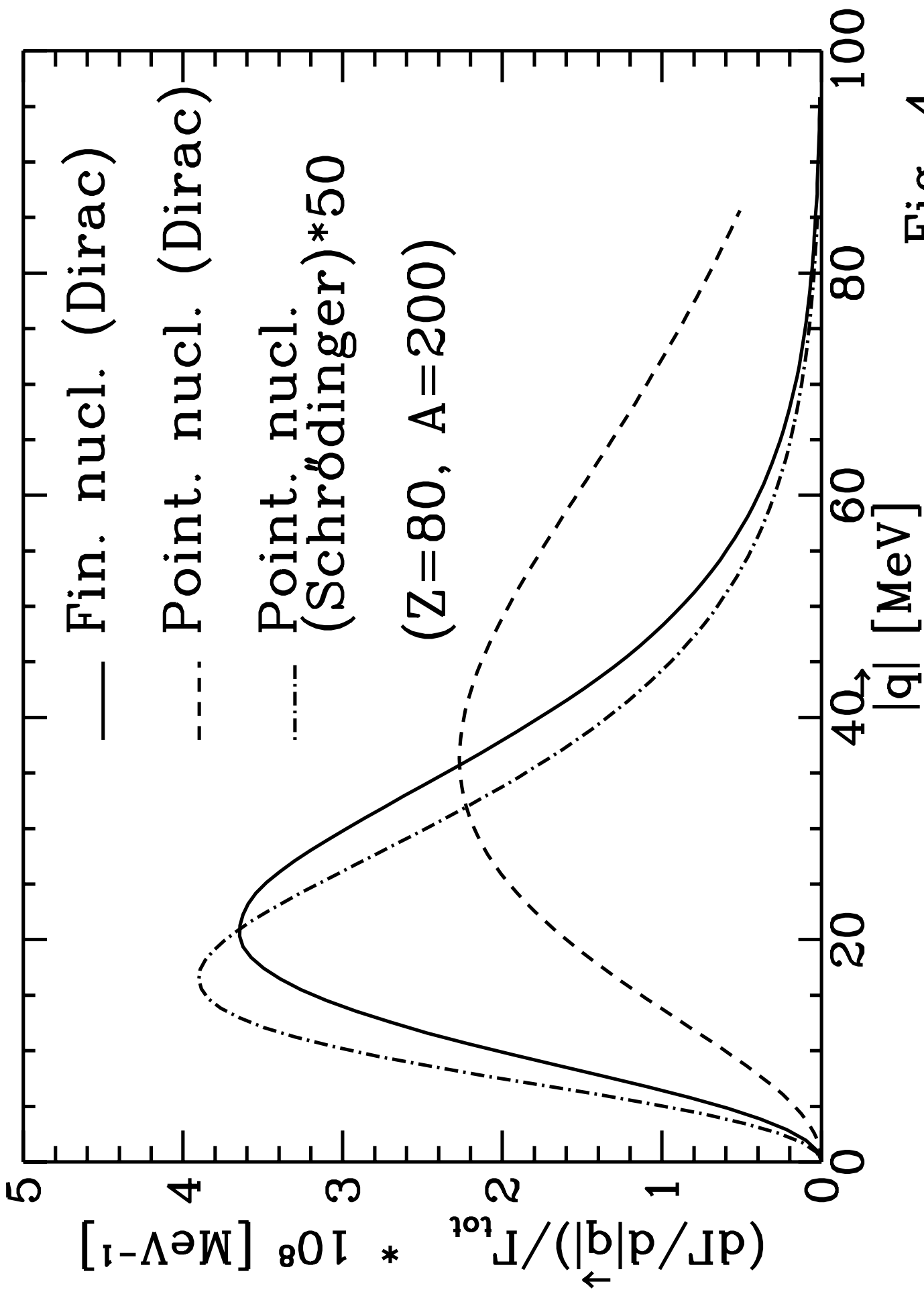


Fig. 4

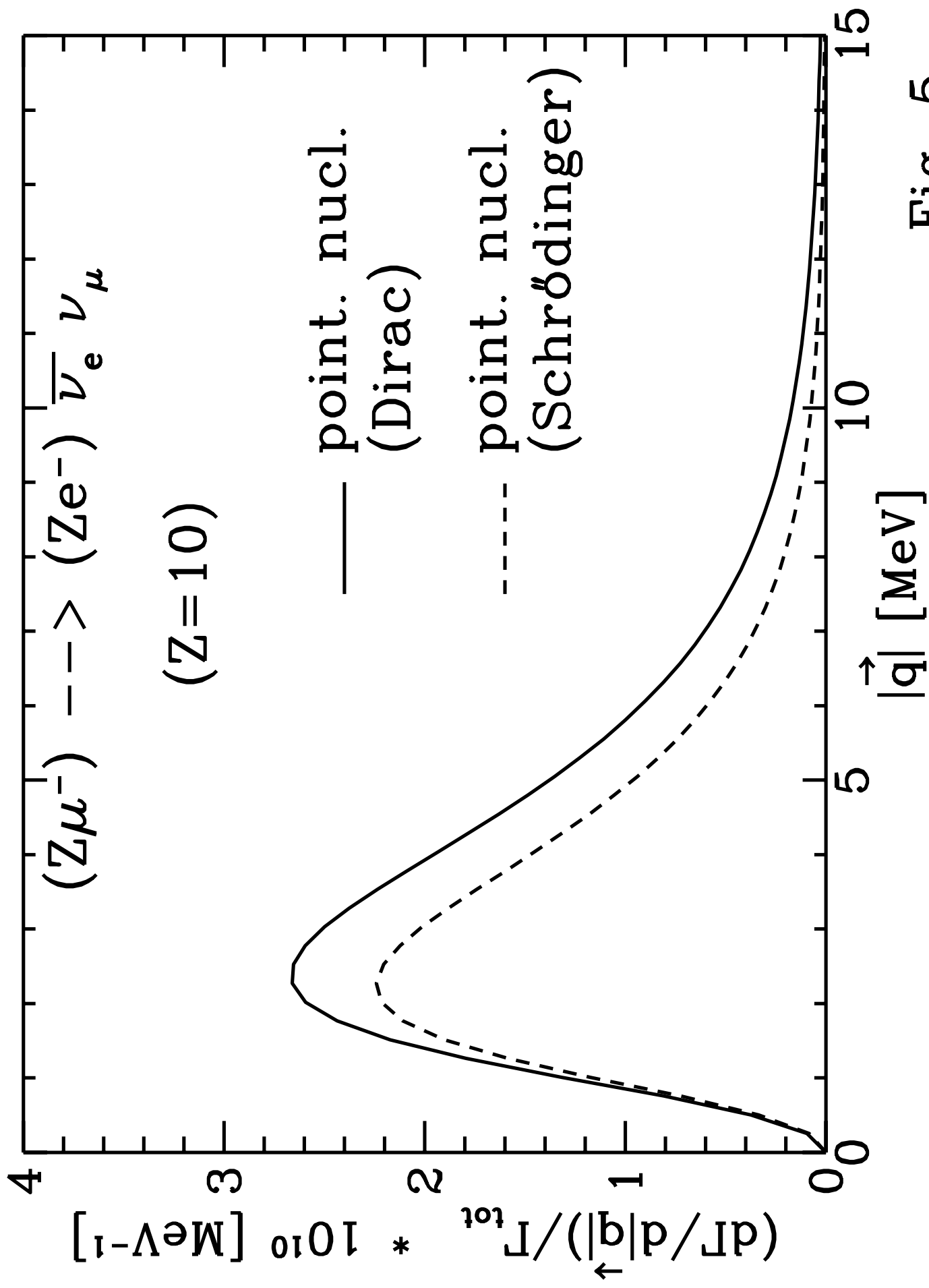


Fig. 5

This figure "fig1-1.png" is available in "png" format from:

<http://arxiv.org/ps/hep-ph/9405230v1>

This figure "fig1-2.png" is available in "png" format from:

<http://arxiv.org/ps/hep-ph/9405230v1>

This figure "fig1-3.png" is available in "png" format from:

<http://arxiv.org/ps/hep-ph/9405230v1>

This figure "fig1-4.png" is available in "png" format from:

<http://arxiv.org/ps/hep-ph/9405230v1>

This figure "fig1-5.png" is available in "png" format from:

<http://arxiv.org/ps/hep-ph/9405230v1>